

Pulsed-laser deposition of high- k titanium silicate thin films

Cite as: J. Appl. Phys. **98**, 054912 (2005); <https://doi.org/10.1063/1.2039274>

Submitted: 29 December 2004 • Accepted: 28 July 2005 • Published Online: 12 September 2005

D. Brassard and M. A. El Khakani



View Online



Export Citation

ARTICLES YOU MAY BE INTERESTED IN

[Tuning the electrical resistivity of pulsed laser deposited TiSiO_x thin films from highly insulating to conductive behaviors](#)

Applied Physics Letters **84**, 2304 (2004); <https://doi.org/10.1063/1.1688999>

[High- \$k\$ titanium silicate thin films grown by reactive magnetron sputtering for complementary metal-oxide-semiconductor applications](#)

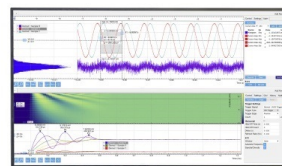
Journal of Vacuum Science & Technology A **22**, 851 (2004); <https://doi.org/10.1116/1.1722530>

[Thermal behavior of the microstructure and the electrical properties of magnetron-sputtered high- \$k\$ titanium silicate thin films](#)

Journal of Applied Physics **103**, 114110 (2008); <https://doi.org/10.1063/1.2937241>

Challenge us.

What are your needs for periodic signal detection?



Zurich
Instruments



Pulsed-laser deposition of high-*k* titanium silicate thin films

D. Brassard and M. A. El Khakani^{a)}

*Institut National de la Recherche Scientifique, INRS-Énergie, Matériaux et Télécommunications,
1650 Boulevard Lionel-Boulet, C.P. 1020, Varennes, Québec J3X 1S2, Canada*

(Received 29 December 2004; accepted 28 July 2005; published online 12 September 2005)

We report on the growth of high-*k* titanium silicate (TiSiO₄) thin films by means of the pulsed-laser ablation of a TiO₂/SiO₂ composite target. We present a systematic investigation of the effect of the oxygen background pressure [$P(\text{O}_2)$] and the substrate deposition temperature (T_d) on both the structural and electrical properties of the films. Fourier-transform infrared spectroscopy and x-ray photoelectron spectroscopy analyses revealed the presence of Ti–O–Si bonds in the films, confirming thereby the formation of the titanium silicate phase. In particular, the $P(\text{O}_2)$ is shown to be a key factor for controlling the morphology, the oxygen content, and consequently the electrical properties of the titanium silicate films. Indeed, while the films deposited at $P(\text{O}_2) \geq 50$ mTorr present some porosity, a high roughness, and poor dielectric and breakdown field characteristics, those grown at $P(\text{O}_2) < 10$ mTorr and postannealed (at 600 °C in O₂) are shown to exhibit a dense and smooth microstructure together with excellent dielectric properties. On the other hand, the resistivity of the vacuum-deposited films is found to decrease remarkably when T_d is raised from 20 to 600 °C. Indeed, a strong correlation (over 14 decades) is established between the resistivity of the titanium silicate films and their oxygen content, pointing up the crucial role of their full oxidation. Thus, by identifying the optimal growth conditions, we were able to achieve dense and stoichiometric high-*k* titanium silicate films combining not only a dielectric constant as high as 33 and a dissipation factor as low as 0.01 but also a high breakdown field of 4 MV/cm.
© 2005 American Institute of Physics. [DOI: 10.1063/1.2039274]

I. INTRODUCTION

The continuous reduction of complementary metal-oxide-semiconductor (CMOS) device feature sizes together with the progressive integration of CMOS components in microelectromechanical systems (MEMS) have put an acute demand on the development of new materials that could simultaneously exhibit high capacitance density and low leakage current.^{1–3} To meet such needs, a possible avenue consists of replacing the traditional low dielectric constant SiO₂ ($k=3.9$) by a new dielectric material with a higher permittivity. Over the past years, the prospect of replacing the gate dielectric of metal-oxide-semiconductor field-effect transistors (MOSFETs) has motivated numerous investigations on several high-*k* materials as possible replacement dielectric materials.^{2–11} Among them, the silicate group (i.e., mixtures of SiO₂ and metal oxides) stands out by offering the interesting possibility of combining the low leakage current and the high breakdown field of SiO₂ while keeping a relatively high dielectric constant.^{2,12} In addition, the silicate films, grown under the appropriate conditions, are generally amorphous, reducing thereby both the roughness of the interfaces and the leakage current through grain boundaries.^{2,6,8–11,13,14} Finally, the silicates generally offer both larger band gap and band offset with Si than their metal oxide counterparts,^{6,15,16} which constitute an advantage for the reduction of the tunneling leakage current. As a consequence, silicate materials (such as zirconium, hafnium, and

yttrium silicates^{8–11}) have been recently investigated and shown to be among the most promising materials for the replacement of the gate dielectric of MOSFETs. On the other hand, the dielectric properties of titanium silicate (or TiO₂/SiO₂ mixed oxide) thin films have been astonishingly much less investigated, even if this material offers the possibility to reach dielectric constant values higher than the other candidates in the silicate group.^{17–20} (TiO₂ has indeed the highest dielectric constant of the metal oxide group, with *k* values in excess of 80 being routinely obtained.^{4,21})

The ternary system consisting of mixtures of TiO₂ and SiO₂ is important for applications in a wide variety of domains. For instance, highly dispersed TiO₂ in a SiO₂ matrix has shown very interesting properties for use as catalysts and catalytic support materials.²² Indeed, this material not only benefits from the excellent structural properties of SiO₂ but the interaction of TiO₂ with SiO₂ generates additional catalytic sites compared to pure TiO₂. On the other hand, by mixing TiO₂ and SiO₂, it is possible to vary the refractive index of the composite material from that of SiO₂ (~1.45) to that of TiO₂ (~2.55).^{23,24} This precise control of the refractive index over such a wide range has been used for the fabrication of several optical devices such as passive or active waveguides, antireflective coatings, and notch filters.^{25–27} Thus, the optical properties of titanium silicate and/or TiO₂–SiO₂ multilayer films, deposited using different processes, have been widely investigated.^{23–27} In contrast, only very few papers were reported so far on the electrical properties of titanium silicate thin films. Among these, it is worth mentioning the work of Kamada *et al.*, where they have shown that chemical-vapor-deposited (CVD) films con-

^{a)}Author to whom correspondence should be addressed; electronic mail: elkhakani@emt.inrs.ca

sisting of a mixture of TiO_2 and SiO_2 exhibit good dielectric properties.²⁰ Also, Nishiyama *et al.*¹⁹ reported that the sputtering of a $\text{TiO}_2/\text{SiO}_2$ target in an Ar/O_2 gas mixture followed by a rapid thermal annealing at 800°C leads to nanocrystalline $(\text{TiO}_2)_{1-x}(\text{SiO}_2)_x$ thin films with a leakage current lower than that of TiO_2 . Recently, we have also demonstrated, using either pulsed-laser deposition^{17,28} (PLD) or magnetron sputtering,¹⁸ that titanium silicate films constitute a promising high- k material for dielectric gate and high-voltage CMOS applications. Very recently, Paskaleva *et al.*²⁹ also investigated the electrical properties of metal-organic CVD-grown $\text{Hf}_x\text{Ti}_y\text{Si}_z\text{O}$ films with various Ti/Hf ratios and reported a dielectric constant of as high as 26 for $\text{Ti}_{0.51}\text{Si}_{0.49}\text{O}_2$ films.

Depending on the specific application, titanium silicate thin films have been deposited using a variety of methods including evaporation,^{30–32} CVD,^{20,24,29,33} sputtering,^{14–16,18,19,23,26} sol-gel,^{22,25,34,35} and PLD.^{17,28} Among these deposition techniques, PLD stands out by its unique features, such as the highly energetic aspect of the species involved in the deposition process and the very high instantaneous deposition rate. This generally results in the growth of thin films with superior properties that compare well with those of the bulk material.³⁶ Interestingly, no systematic study has been reported yet on the effect of the deposition conditions on the structural and electrical properties of pulsed-laser deposited titanium silicate thin films.

In this paper, we present a systematic investigation and optimization of the deposition conditions of high- k titanium silicate thin films using the laser ablation of a TiO_2 – SiO_2 composite target. A focus is put here on the effect of both the oxygen background pressure [$P(\text{O}_2)$] and the substrate deposition temperature (T_d) on the morphological, structural, and dielectric properties of the films. It is shown that, by varying the growth and/or postprocessing conditions, one can control the morphology (from highly porous films to dense and compact microstructure), the electrical resistivity (from highly resistive down to fairly conductive), and the dielectric properties of the films. Optimum growth conditions leading to titanium silicate films combining high dielectric constant, low dissipation factor, and high breakdown field are identified.

II. EXPERIMENT

The titanium silicate thin films were deposited by means of pulsed-laser ablation of a 3 in.-diameter $\text{TiO}_2/\text{SiO}_2$ composite target using a pulsed KrF excimer laser operating at a wavelength of 248 nm with a pulse duration of 15 ns and a repetition rate of 30 Hz. It is to be mentioned that a Ti–Si metallic target can also be used to grow titanium silicate films by means of a reactive PLD process, as we previously demonstrated in Ref. 17. However, in comparison with their oxide counterparts, metallic targets emit more droplets (particularly in the case of Si, which affect the electrical properties of the films), absorb less efficiently the UV laser light, and finally were found to produce titanium silicate films with lower k values.¹⁷ The pressed powder target was composed of an equal atomic ratio of TiO_2 and SiO_2 powders (purity of

99.9%) and was simultaneously rotated and translated across the laser beam during the deposition to ensure a uniform erosion of the target surface. The laser was focused on the target at an incident angle of 45° and at a fluence of $\sim 2\text{ J}/\text{cm}^2$. Before each deposition, the target was cleaned by laser ablating its surface for about 10 min while isolating the substrate from the ablated species by a shutter. The films were deposited onto different substrates, namely, (i) (100)-oriented undoped silicon wafers, (ii) fused silica disks, and (iii) platinum-coated Si wafers (consisting of a Pt/Ti/SiO₂/Si structure). The substrates were conventionally cleaned, mounted on a substrate holder, and placed parallel to the target at a perpendicular distance of 6.5 cm. The substrate holder assembly was animated by a rotation motion during the deposition to ensure thickness uniformity. The substrate deposition temperature (T_d) was controlled in the 20 – 600°C range using a resistive heater beneath the substrate and was measured using a calibrated thermocouple embedded in the substrate holder. Prior to the deposition, the chamber was first turbopumped to a base pressure of about 2×10^{-5} Torr. Films were then deposited either under vacuum (2×10^{-5} Torr) or under a specific oxygen pressure [$P(\text{O}_2)$] ranging from 1 to 100 mTorr obtained by filling the deposition chamber with high-purity (99.995%) oxygen. Postdeposition annealings were performed by placing the films in a quartz tube furnace at a temperature of 600°C in O_2 for 30 min.

The composition and chemical bonding states of the PLD titanium silicate films were investigated by means of x-ray photoelectron spectroscopy (XPS) using the Al $K\alpha$ monochromatic radiation (1486.6 eV) of an ESCALAB 200I-XL spectrophotometer after a systematic *in situ* surface cleaning by means of 5 keV Ar^+ ion sputtering. Both Fourier-transform infrared (FTIR) spectroscopy and micro-Raman spectroscopy were used to further characterize the films bonding states. A BOMEM-Michelson-100 spectrometer was used for the FTIR analyses (performed in the 300 – 4000 cm^{-1} range) while a Renishaw imaging microscope wire (argon-ion excitation $\lambda=514.5\text{ nm}$) was used for the Raman measurements. The crystalline structure of the films was investigated using x-ray diffraction (XRD) at a grazing incident angle of 1° (Philips X'pert-MPD x-ray diffractometer), while their surface morphology was characterized by means of both scanning electron microscopy (SEM) and atomic force microscopy (AFM). The thickness of the films was in the 150 – 350 nm range, as determined from both Dektak-3030 profilometer measurements and cross-section SEM observations.

For the electrical and dielectric characterizations of the films, metal-insulator-metal (MIM) capacitors consisting of a Pt/silicate/Pt/Ti/SiO₂/Si multilayer structure were fabricated. The electrical resistivity of the films was calculated from the low-field ($E < 50\text{ kV}/\text{cm}$) Ohmic conduction region of the current-voltage characteristics of the MIM capacitors. On the other hand, the room-temperature resistivity of the films showing a conductive behavior (resistivity $< 10^5\ \Omega\text{ cm}$) was investigated using the conventional four-point probe method. The breakdown fields (E_{bd}) of the films were measured by slowly ramping up the voltage ap-

plied on the films until breakdown, characterized by a sudden rise in current, is observed. The dielectric properties, such as the dielectric constant ϵ and dissipation factor $\tan \delta$, were obtained from the complex impedance characterization of the MIM capacitors in the 1 kHz–10 MHz frequency range using a HP-4192A impedance analyzer. Oscillation voltage was set at 50 mV, no bias voltage was applied, and a calibration was performed to remove parasite series impedance.

III. RESULTS AND DISCUSSION

The effects of the substrate deposition temperature T_d , oxygen pressure $P(O_2)$, and postdeposition annealing on the morphology, chemical bondings, and electrical properties of pulsed-laser deposited titanium silicate thin films are discussed next.

A. Morphology

The morphology of the deposited titanium silicate thin films is found to change drastically with both $P(O_2)$ and T_d . SEM observations reveal that the films deposited at low oxygen pressures [$P(O_2) \leq 10$ mTorr] exhibit a dense microstructure without any apparent porosity [as that shown in Fig. 1(a)], regardless of the value of T_d in the 20–600 °C range. As $P(O_2)$ is increased to 50 mTorr and beyond [Figs. 1(b) and 1(c)], not only the films become more and more porous but also their features significantly increase in size. Indeed, at 100 mTorr and $T_d=20$ °C, the films have a highly porous structure and are composed of very large (~200 nm) features [note the lower magnification for the cross-section of Fig. 1(c)]. However, the high porosity of the films deposited at high $P(O_2)$ is found to reduce drastically with the increase of T_d . Indeed, at $T_d=600$ °C the films deposited under 100 mTorr exhibited a much denser and smoother structure [see Fig. 1(d)]. However, some vertical porosity can still be seen in the cross-section view of Fig. 1(d). These results show that denser films can be obtained at high deposition temperature and low gas pressure, in good accordance with the results reported on coevaporated TiO_2 – SiO_2 films.³¹

The results of the AFM characterizations of the titanium silicate films corroborate well with the above-discussed SEM characterization. Indeed, as shown in Fig. 2, the measured rms roughness of the films deposited at low pressures (vacuum and 1 mTorr) is very low (~0.1 nm). At pressures between 1 and 10 mTorr, the roughness of the films begins to increase and a very high rms roughness of about 20 nm is obtained for $P(O_2)=100$ mTorr and $T_d=20$ °C. However, it is noteworthy that the roughness of the films deposited at 100 mTorr can be reduced significantly, down to a value of ~2 nm, by increasing T_d to 600 °C. On the other hand, subjecting the films to a postdeposition annealing at 600 °C for 30 min was found to have almost no effect on the morphology and roughness of the films.

The large variations of both the morphology and roughness of the titanium silicate thin films with the background oxygen pressure suggest that the energy of the particles arriving at the substrate during deposition is a key parameter

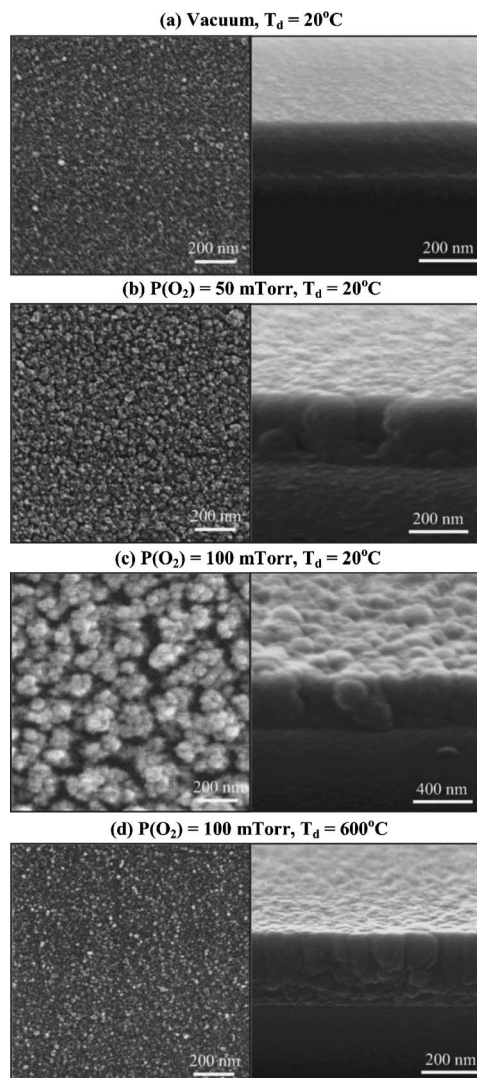


FIG. 1. SEM micrographs of PLD titanium silicate thin films deposited on silicon substrate showing, respectively, top and cross-sectional views on the left-hand and right-hand columns. The films were deposited under the following $P(O_2)$ and T_d : (a) vacuum and 20 °C, (b) 50 mTorr and 20 °C, (c) 100 mTorr and 20 °C, and (d) 100 mTorr and 600 °C.

in the formation of dense silicate films. Indeed, the laser ablation of the target in the PLD process is well known to eject highly energetic species, which favors the formation of dense films when the deposition is performed under a high-vacuum environment.³⁶ On the other hand, under higher background pressures, the ablated species undergo several collisions with the oxygen molecules and thus arrive at the substrate with a much lower energy, which limits their surface mobility and consequently leads to a porous structure. It is noteworthy that the abrupt takeoff of the roughness of the films (Fig. 2) at 10 mTorr coincides with the gas pressure at which the mean free path of the ablated species is comparable to the target-substrate distance. Finally, at higher T_d , the enhanced mobility of the atoms at the surface of the growing film compensates, to a certain extent, for the slowing down of the species in the background gas and leads to relatively dense and smooth surface morphologies.

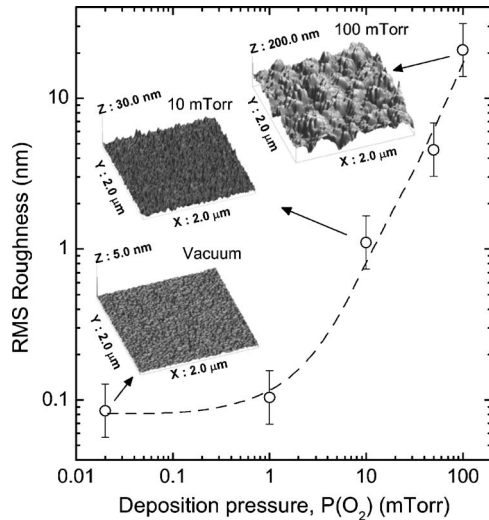


FIG. 2. AFM roughness analysis of PLD titanium silicate thin films deposited at $T_d=20^\circ\text{C}$. Insets show three-dimensional (3D) views of $2\times 2\ \mu\text{m}$ micrographs for films deposited under vacuum and at $P(\text{O}_2)=10$ and $100\ \text{mTorr}$.

B. Microstructure and chemical bondings

Figure 3(a) shows a typical XRD spectrum obtained for the PLD titanium silicate thin films, regardless of their T_d or $P(\text{O}_2)$. No diffraction peak is observed in the XRD spectra even after a postannealing treatment at 600°C , indicating thereby that all the PLD titanium silicate thin films investi-

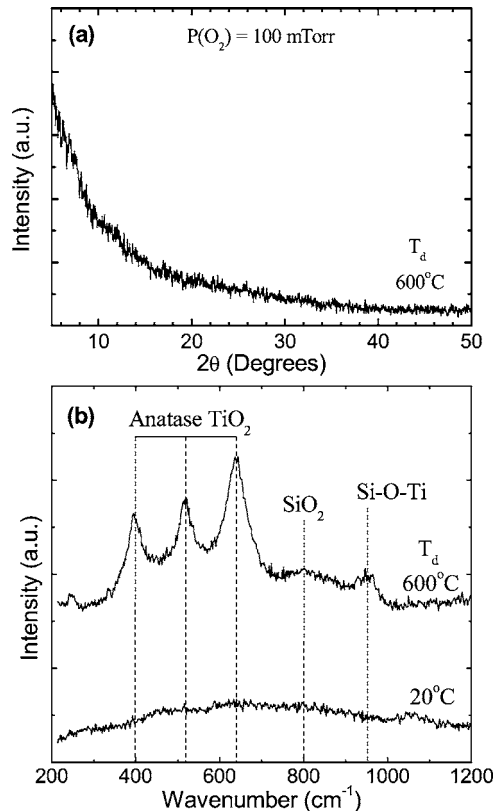


FIG. 3. (a) Grazing angle XRD spectrum of a PLD titanium silicate thin film deposited at $T_d=600^\circ\text{C}$ and $P(\text{O}_2)=100\ \text{mTorr}$. (b) Raman spectra of PLD titanium silicate thin films deposited at $100\ \text{mTorr}$ under substrate deposition temperatures of 20 and 600°C .

gated in the present work are amorphous. This is not surprising when recalling that the introduction of SiO_2 into a TiO_2 matrix can prevent crystallization,^{30,31} even if pure TiO_2 films are known to transform from amorphous to the crystalline anatase at temperatures as low as 300°C and to the rutile structure at temperatures in the $600\text{--}700^\circ\text{C}$ range.^{30–33,35–37} Indeed, e-beam-evaporated titanium silicate films with intermediate compositions (i.e., Ti/Si atomic ratio of ~ 1) have been reported to remain amorphous at temperatures of up to 600°C ,^{30,31} in agreement with our present results. Nevertheless, Raman spectroscopy analyses have revealed, in the sole case of the films deposited at 600°C , the presence of some weak absorption bands [Fig. 3(b)], which could be associated with the beginning of some precipitation of anatase nanocrystals. Indeed, the three bands centered around 399 , 516 , and $640\ \text{cm}^{-1}$, respectively, are indicative of the presence of TiO_2 anatase crystallites in the films.^{21,22} The other two broad and weak bands located at 800 and $960\ \text{cm}^{-1}$ are due to the presence of SiO_2 and to Ti–O–Si type of bondings, respectively.²² One should, however, recall that Raman spectroscopy is extremely sensitive to the presence of titania crystallites due to the enhanced scattering associated with crystalline boundaries (the minimum detectable amount in $\text{TiO}_2\text{--SiO}_2$ mixed oxides has been reported to be as low as $0.05\ \text{wt}\%$).^{22,38} As a consequence, combining the XRD and Raman results, one can conclude that the PLD titanium silicate films deposited at 600°C are predominantly amorphous with the presence of very few anatase crystallites. (Such TiO_2 precipitates are highly likely too small in size and too low in quantity to yield a detectable XRD signal.) For $T_d < 600^\circ\text{C}$, the films are totally amorphous since neither XRD nor Raman spectroscopy revealed the presence of any peak in the spectra.

On the other hand, FTIR spectroscopy characterizations brought some additional insights on the local environments of Ti, Si, and O atoms in the PLD titanium silicate films as their growth conditions are varied. Indeed, Fig. 4 reveals the presence of the absorption band located around $930\ \text{cm}^{-1}$, which is due to the presence of Ti–O–Si bonds (i.e., Si–O–stretching vibration in Si–O–Ti⁴⁺ local environment).^{22,35,39} The presence of this band, regardless of the deposition conditions and annealing treatments, confirms that the original constituents of the target (namely, SiO_2 and TiO_2 powders) were atomically mixed during the laser ablation deposition process to form the titanium silicate phase. Also one can note the presence of the transverse-optical (TO_1) asymmetric stretching vibration of the Si–O–Si bonds located at about $1050\ \text{cm}^{-1}$ and its shoulder located in the $1100\text{--}1200\ \text{cm}^{-1}$ region [composed of the TO_2 and longitudinal-optical LO_2 modes; see the deconvolution shown in Fig. 4(a)].⁴⁰ One should note that, while the position of the Si–O–Si band appears in the $1070\text{--}1080\ \text{cm}^{-1}$ range for pure SiO_2 ,⁴⁰ it is normally found at $\sim 1050\ \text{cm}^{-1}$ for equimolar $\text{SiO}_2\text{--TiO}_2$ mixed oxides,^{35,39} as a result of the disruption of the Si–O–Si network by the presence of neighboring titanium atoms.³⁹ The Si–O–Si asymmetric bending vibrational band is also observed at $\sim 800\ \text{cm}^{-1}$ along with a peak, which is located in the $350\text{--}500\ \text{cm}^{-1}$ region (not shown here), corresponding either to the Si–O–Si asymmetric rocking or indicating the

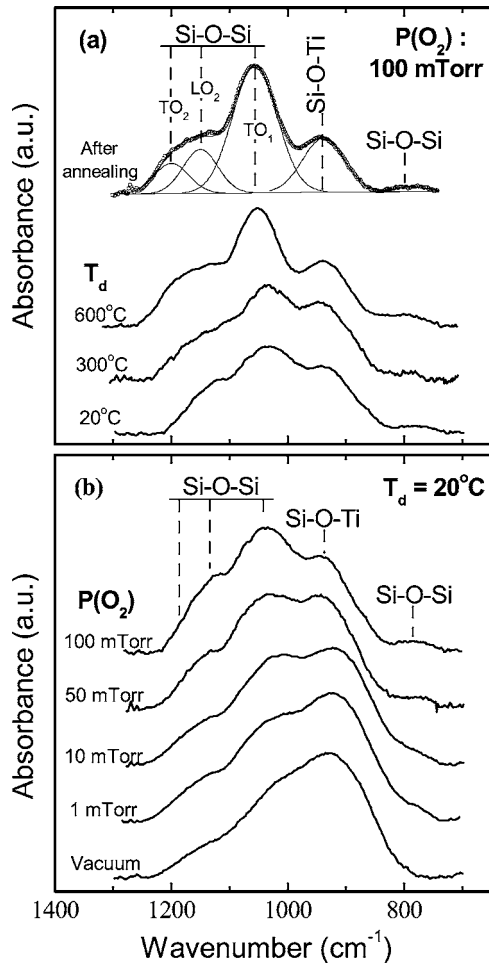


FIG. 4. FTIR absorbance spectra of the PLD titanium silicate films in the 700–1300 cm^{-1} wave number range: (a) effect of the T_d and postdeposition annealing for films deposited at $P(\text{O}_2)=100$ mTorr and (b) effect of $P(\text{O}_2)$ on films deposited at $T_d=20^\circ\text{C}$.

presence of Ti–O bonds.^{39,40} Finally, the films having a porous microstructure [such as those shown in Fig. 1(c)] were found to exhibit a weak absorption band around 3400 cm^{-1} , which indicates the presence of some adsorbed moisture and/or silanol Si–OH groups.^{35,40} In contrast, no moisture and/or Si–OH-related absorption band was detected in the films having a dense microstructure [such as that shown in Fig. 1(a)].

By deconvoluting the 700–1300- cm^{-1} region of the FTIR spectra into its corresponding vibrational modes [see Fig. 4(a)], we were able to point out the three following points: (i) first, at $P(\text{O}_2)=100$ mTorr, the increase of T_d from 20 to 600 $^\circ\text{C}$ is found to lead to significant increase of the relative proportion of the TO_1 mode of the Si–O–Si band to the detriment of the Si–O–Ti band. This phenomenon is seen to be more pronounced at $T_d=600^\circ\text{C}$ and is further enhanced when the films are subjected to the postannealing treatment [upper spectrum of Fig. 4(a)]. Such a decrease in the Ti–O–Si band intensity at $T_d=600^\circ\text{C}$ could be explained by some segregation that starts to take place leading to the formation of SiO_2 -rich and TiO_2 -rich environments along with some TiO_2 crystallites precipitation, as revealed by the above-discussed Raman results; (ii) second, the increase of T_d (or the annealing treatment) was found to be accompanied

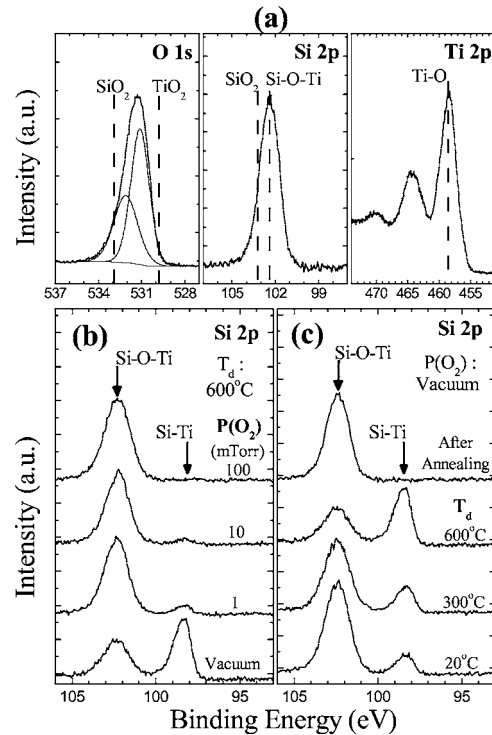


FIG. 5. High-resolution XPS spectra of the PLD titanium silicate thin films: (a) typical O_{1s} , Si_{2p} , and Ti_{2p} core-level spectra for films deposited in vacuum at $T_d=600^\circ\text{C}$ and postannealed at 600 $^\circ\text{C}$, (b) effect of $P(\text{O}_2)$ on the Si_{2p} line for films deposited at $T_d=600^\circ\text{C}$, and (c) effect of the T_d and postdeposition annealing on the Si_{2p} line for films deposited under vacuum.

by a narrowing of both Si–O–Si and Si–O–Ti bands (from 110 to 80 cm^{-1}), which is a clear indication of some local ordering taking place in the films as T_d is increased; and (iii) finally, at $T_d=20^\circ\text{C}$, the increase of $P(\text{O}_2)$ from vacuum to 100 mTorr is found to provoke a noticeable increase of the Si–O–Si component to the detriment of Ti–O–Si type of local environments [Fig. 4(b)]. Also, some peak narrowing (from 130 to 110 cm^{-1}) was also observed as $P(\text{O}_2)$ is increased. These both results suggest that, at higher $P(\text{O}_2)$, the ablated species arriving on the substrate have less energy than in vacuum, leading thereby to some sort of “soft-landing” which would, on one hand, provoke less disorder (narrower peaks) and, on the other hand, less atomic mixing, reducing thereby the formation of Ti–O–Si type of environments.

Figure 5(a) shows the typical O_{1s} , Si_{2p} , and Ti_{2p} core-level XPS spectra of the PLD titanium silicate thin films. The oxygen O_{1s} spectrum is found to consist of a single peak at a position (~ 531.5 eV), which is in between that of O_{1s} in SiO_2 (532.7 eV) and in TiO_2 (529.7 eV),^{41,42} confirming once again the presence of Ti–O–Si type of environments in the films. (The absence of any peak at 529.7 eV suggests that the content of TiO_2 crystallites is very weak and definitely below the sensitivity of the XPS technique.) On the other hand, as seen in Fig. 5(a), the O_{1s} peak of the film deposited at $T_d=600^\circ\text{C}$ is relatively large [full width at half maximum (FWHM) ~ 2.1 eV] and slightly asymmetric. Hence, this photoelectron peak can be deconvoluted with at least two peaks [centered around 531.1 and 532.1 eV, respectively, see Fig. 5(a)] that could account for the presence of two types of

silicate environments (i.e., slightly SiO_2 -rich and slightly TiO_2 -rich). This might be interpreted as an indication that some segregation is beginning to take place in the films deposited or annealed at 600°C , in agreement with the FTIR results. The Si_{2p} peak appears at a binding energy of 102.4 eV, compared to 103.3 eV in pure SiO_2 .⁴¹ This decrease in the binding energy of Si_{2p} compared to SiO_2 is commonly observed in various types of silicates^{10–12,41,42} and results from a decrease of the effective positive charge on the Si atoms due to the formation of Ti–O–Si bonds. Also, the $\text{Ti}_{2p_{3/2}}$ peak position (458.4 eV) is found to be very consistent with the presence of Ti^{4+} into Ti–O–Si type of environments.⁴¹ Finally, using the appropriate sensitivity factor, the composition of the films was measured. Within the error of the measurement, the Ti/Si ratio of all the PLD titanium silicate films is found to be of about 1.

Figure 5(b) shows the effect of $P(\text{O}_2)$ on the Si_{2p} core level. For the films deposited in vacuum, the Si_{2p} spectra show, in addition to the peak corresponding to Ti–O–Si (at ~ 102.4 eV), the presence of a second peak located at about 98.6 eV. This peak is clearly seen to reduce drastically as $P(\text{O}_2)$ is increased and disappears for $P(\text{O}_2) \geq 50$ mTorr. Conversely, Fig. 5(c) shows, for the films deposited in vacuum, that the 98.6 eV peak increases to the detriment of the Ti–O–Si peak as T_d is increased from 20 to 600°C . However, after 30 min of annealing at 600°C in O_2 , the 98.6 eV peak completely disappears and only the Ti–O–Si-related peak is present. The 98.6 eV peak indicates the presence of metallic bonds, such as Si–Ti [98.7 eV (Ref. 43)], in the films. In addition, the analysis of the Ti_{2p} core levels (not shown here, see Ref. 28) has confirmed the presence of Ti–Si metallic bondings together with some titanium suboxides (Ti_2O_3 and/or TiO) particularly in the films deposited at $T_d = 600^\circ\text{C}$.

The presence of Ti–Si bonds and titanium suboxides in the titanium silicate films suggests some lack of oxygen in the films. Indeed, the XPS calculated $[\text{O}]/([\text{Si}]+[\text{Ti}])$ oxygen atomic ratio was found to be as low as 1.2 for the films deposited at $T_d = 600^\circ\text{C}$ in vacuum. On the other hand, the oxygen atomic ratio is of about 2 for the films deposited at high $P(\text{O}_2)$ or postannealed under O_2 . Thus, depending on the deposition conditions, films having a composition ranging from fully oxygenated silicates (i.e., TiSiO_4) down to strongly oxygen-depleted silicates (i.e., $\text{TiSiO}_{2.5}$) are obtained. The oxygen deficiency observed in the films deposited in vacuum is thought to be due to some recombination of the ablated oxygen atoms during the laser ablation process and/or to thermally induced oxygen desorption from the film surface during its growth at high T_d in a high-vacuum environment. Thus, by providing extra oxygen atoms [either through postannealing under oxygen atmosphere or deposition under sufficiently high $P(\text{O}_2)$] to the films, they recover their fully oxidized state and no Ti–Si metallic bonding is present anymore. It is worth discussing here that what we refer to as “vacuum” is a residual base pressure of 2×10^{-5} Torr, which is highly likely caused, to a large extent, by the presence of some residual moisture in the vacuum system. However, it is important to notice that a residual pressure of $\sim 10^{-5}$ Torr remains very negligible in compari-

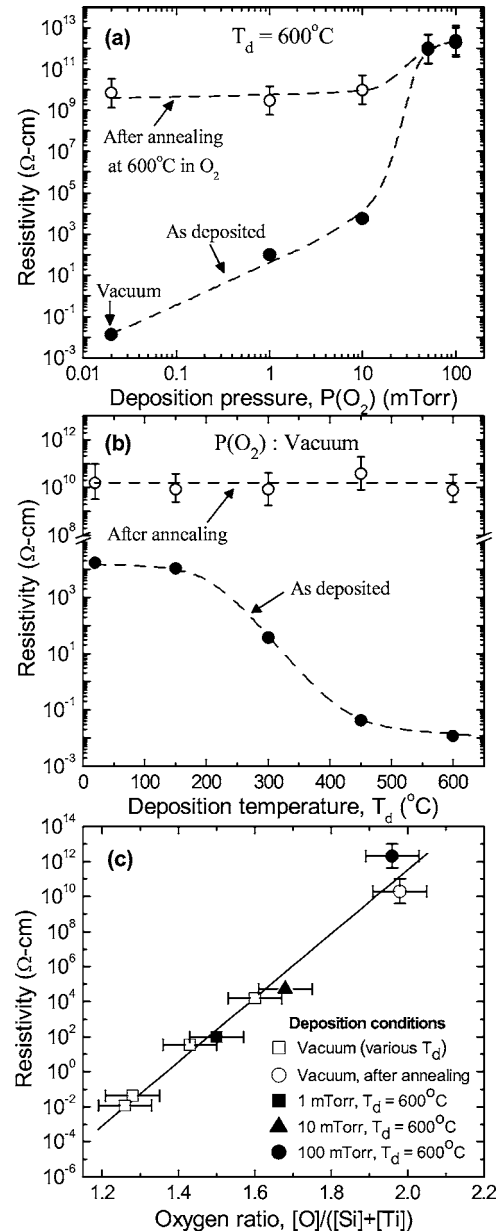


FIG. 6. Room-temperature resistivity of the PLD titanium silicate thin films. (a) Effect of the oxygen background pressure ($T_d = 600^\circ\text{C}$) and (b) effect of the substrate deposition temperature (films deposited under vacuum) both before and after postdeposition thermal annealings at 600°C in O_2 . (c) Cross-plot showing the variation of the resistivity of the titanium silicate films as a function of their oxygen atomic content.

son with the O_2 background pressures investigated in the present work (from approximately two to four orders of magnitude larger than the base pressure). As a consequence, even if some oxygen uptake might occur at the base pressure of 2×10^{-5} Torr, its amount will be definitely negligible in comparison with the oxygenation (and its effect on film properties) caused by the intentional introduction of O_2 in the 1–100-mTorr range. In fact, an increase of the background pressure even to 10^{-4} Torr would induce a resistivity change of approximately one order of magnitude, which remains negligible in comparison with the 14 orders-of-magnitude variation caused by increasing the partial oxygen pressure from 2×10^{-5} Torr to 100 mTorr [see Fig. 6(a)].

C. Electrical properties

The electrical properties of the PLD titanium silicate thin films were observed to change considerably depending on their growth conditions. Figure 6(a) shows the effect of $P(O_2)$ on the room-temperature resistivity (ρ) of the films deposited at $T_d=600$ °C. Before annealing, the resistivity is found to be surprisingly low for $P(O_2) < 50$ mTorr (ρ as low as 1.2×10^{-2} Ω cm) when one considers that the target material is composed of two highly resistive compounds (TiO₂ and SiO₂). On the other hand, the resistivity is seen to increase rapidly when $P(O_2)$ is increased [with a marked increase of approximately nine orders of magnitude when $P(O_2)$ is varied from 10 to 50 mTorr] and highly insulating films with a resistivity of about 10^{12} Ω cm are obtained for $P(O_2) \geq 50$ mTorr. The postannealing treatment is also found to increase dramatically the resistivity of the films deposited at low $P(O_2)$, while it has nearly no effect on those deposited at $P(O_2) \geq 50$ mTorr. Thus, Fig. 6(a) shows that the resistivity of the films can be varied over a range as wide as 14 orders of magnitude by simply changing the background pressure from vacuum to 100 mTorr of O₂. The deposition temperature is also found to affect significantly the resistivity of the films [Fig. 6(b)]. Indeed the resistivity of the films deposited under vacuum is shown to decrease from 1.6×10^4 to 1.2×10^{-2} Ω cm when T_d is increased from 20 to 600 °C. Also, the postannealing treatment is found to increase the resistivity of the films by several orders of magnitude reaching a high-resistivity level of $\sim 10^{10}$ Ω cm, regardless of the initial T_d .

By analyzing these very large resistivity variations in the light of the above discussed XPS results, it clearly arises that all the films exhibiting a resistivity lower than 10^6 Ω cm contain Ti–Si metallic bondings and are oxygen depleted. It is worth recalling that both titanium silicides and titanium suboxides are quite conductive with resistivities of $\sim 1.5 \times 10^{-5}$ Ω cm for TiSi₂,⁴⁴ $\sim 10^{-2}$ for Ti₂O₃, and 2×10^{-4} Ω cm for TiO.^{45,46} Thus, the presence in the films of such conductive bondings and the variation of their content are at the origin of the observed resistivity variations. On the other hand, when the films are fully oxygenated [either deposited at high $P(O_2)$ or subjected to the postannealing treatment] they exhibit a highly insulating behavior. These results emphasize the crucial role of oxygen incorporation in the titanium silicate films in determining their electrical behavior. Figure 6(c) demonstrates well such a strong correlation between the resistivity of the PLD titanium silicate films and their oxygen content. Indeed, the resistivity of the titanium silicate films is seen to vary in a strikingly exponential way with their oxygen content (over a resistivity range as wide as 14 decades). Such a remarkable exponential dependence over such a wide range suggests that the conduction of these films would obey a mechanism involving tunneling between local conducting environments.⁴⁷

Figure 7 shows the frequency dependence of the dielectric constant as a function of T_d for the titanium silicate thin films deposited under vacuum and postannealed at 600 °C. First, these films are found to exhibit a high dielectric constant k in the 21–33 range. It is noteworthy that the dielectric

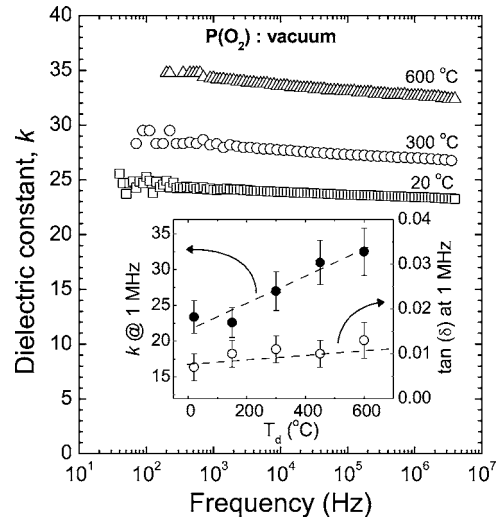


FIG. 7. Variation of the dielectric constant with frequency of PLD titanium silicate thin films deposited under vacuum after postannealing at 600 °C in O₂. Inset shows the variation of both the dielectric constant and the dissipation factor $\tan \delta$ as a function of the substrate deposition temperature.

constant of such films is much higher than those normally obtained for Zr, Hf, or Y silicate where k is rather in the 10–15 range.^{2,6,8,10–12} Also, the permittivity showed no appreciable dispersion with frequency over all the 1 kHz–10 MHz frequency range, indicating that the electrical properties of the films are not affected by ionic space-charge carriers or electrode barrier effects.^{48,49} In addition, the inset of Fig. 7 shows that while the films exhibit an almost invariable low dissipation factor of about 0.01, their dielectric constant is seen to increase significantly from 21 to 33 when T_d is raised from 20 to 600 °C. Such an increase of k with T_d seems to be similar to what is generally observed for oxide films (such as TiO₂ films for which k has been reported to increase when the films are exposed to higher temperatures due to the improvement of their crystallinity^{4,21}). In the case of our amorphous PLD titanium silicate films, it is believed that the increase of k with T_d could result from an increase of the local order in the films, as revealed by FTIR measurements.

The films deposited at $P(O_2) \geq 50$ mTorr were found to exhibit different dielectric properties compared with those deposited under vacuum. Indeed, Fig. 8(a) shows the frequency dependence of k for PLD titanium silicate films deposited under $P(O_2)=50$ mTorr and $T_d=600$ °C (both before and after thermal annealings). It is clearly seen that these films exhibit an important dielectric dispersion in the investigated frequency range. At low frequencies, the k value is very high (~ 250), but it considerably reduces as the frequency is increased to reach a value that is similar to those of the films deposited under vacuum (i.e., $\epsilon \sim 20$). Also, Fig. 8(b) shows that the dissipation factor is very high and presents a peak with a maximum of about 0.6 centered around a frequency of ~ 50 kHz. The postdeposition annealing at 600 °C is found to shift slightly the relaxation toward lower-frequency values and to lower slightly the intensity of the dissipation factor peak. A similar but more intense relaxation was also observed for the films deposited at 100 mTorr (not

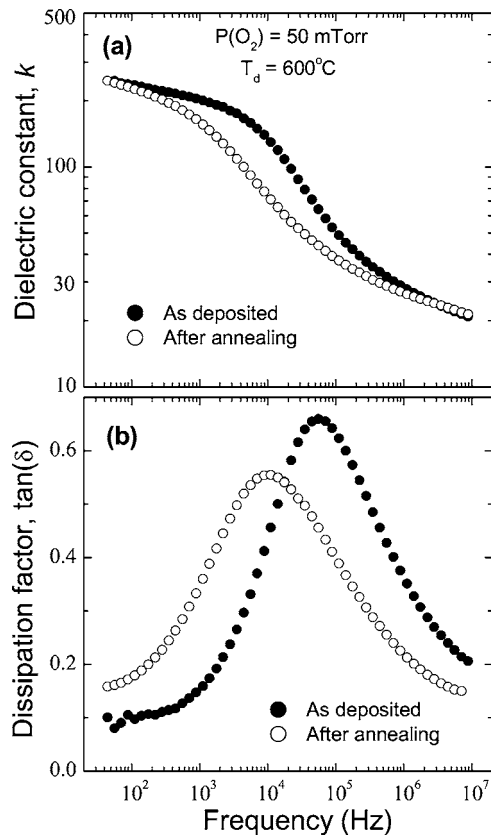


FIG. 8. Variation of (a) the dielectric constant and (b) the dissipation factor with frequency of PLD titanium silicate thin films deposited at $P(O_2) = 50$ mTorr and $T_d = 600^\circ\text{C}$ both before and after the postannealing treatment at 600°C in O_2 .

shown here). Thus, these rather poor dielectric properties of the films deposited at $P(O_2) \geq 50$ mTorr are thought to be a consequence of their porous structure (as revealed by SEM and AFM characterizations) which tends to absorb moisture (as also shown by the FTIR measurements). Indeed, the presence of adsorbed water molecules or Si–OH in porous dielectric films has a direct influence on the concentration of H^+ -ion charge carriers which, in turn, affects their polarisability.^{48,50}

Figure 9(a) shows the effect of the deposition temperature on the breakdown field E_{bd} for PLD titanium silicate films deposited both under vacuum and at $P(O_2) = 100$ mTorr. A high E_{bd} of about 3.9 ± 0.2 MV/cm is obtained for the films deposited under vacuum, without any significant variation with T_d . The breakdown field of those titanium silicate films is naturally found to be higher than the values quoted for either rutile-type TiO_2 films (in the 0.5–1.0-MV/cm range³⁷) or for amorphous TiO_2 [$E_{bd} = 2.7$ MV/cm (Ref. 21)]. On the other hand, for the films deposited at $P(O_2) = 100$ mTorr, E_{bd} is found to improve markedly when T_d is increased from 20 to 600°C . This increase of the breakdown field with T_d , in conjunction with the higher breakdown of the films deposited under vacuum, suggest that the porosity of the films directly affects their resistance to breakdown. Indeed, as suggested from the SEM observations (Fig. 1), while dense and compact structure is obtained at low $P(O_2)$, the porosity of films deposited at high $P(O_2)$ is found to reduce with T_d . In order to further inves-

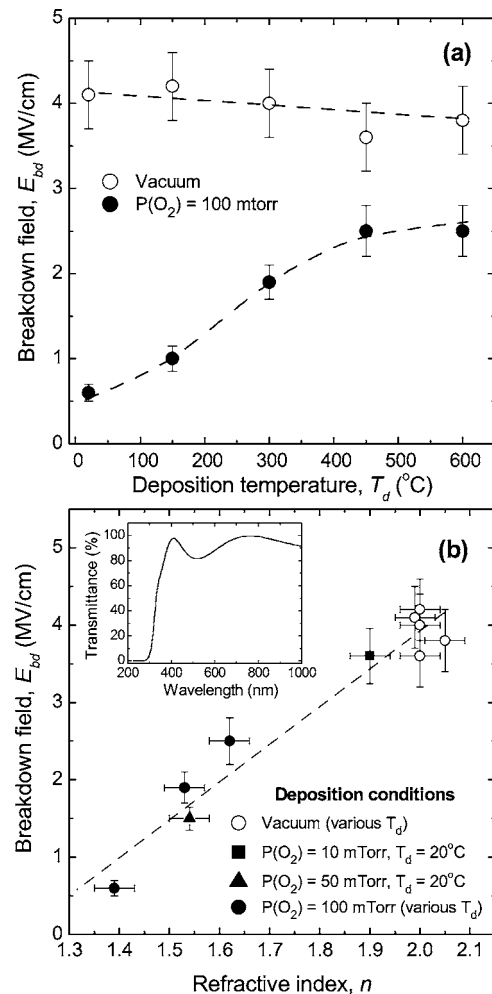


FIG. 9. (a) Effect of the T_d on the breakdown voltage for films deposited at $P(O_2) = 100$ mTorr (closed circles) and under vacuum (open circle) after their postannealing in O_2 . (b) Cross-plot of the breakdown field of the titanium silicate films as a function of their corresponding refractive index. The inset shows a typical transmittance measurement of a titanium silicate films deposited on a fused silica substrate.

tigate the relationship between the breakdown field and the porosity (or the density) of the films, the refractive index of the films was measured from transmittance measurements [a typical transmittance curve is shown in the inset of Fig. 9(b)]. It is worth recalling here that the refractive index n of a material can be assumed to vary linearly with its density ρ (i.e., $\rho \sim n - 1$) according to the first-order rule of mixing.⁵¹ Thus, as shown in Fig. 9(b), the films deposited under vacuum were found to exhibit a refractive index of ~ 2.0 , regardless of their T_d . The refractive index of titanium silicate films with a Ti/Si molar ratio of 1 is reported to be in the 1.9–2.0 range,^{23,41} which thus indicates the high density and very low porosity of our PLD silicate films deposited under vacuum. On the other hand, as $P(O_2)$ is increased, the refractive index is found to reduce drastically to reach ~ 1.4 for the films deposited at $P(O_2) = 100$ mTorr and $T_d = 20^\circ\text{C}$ and to ~ 1.6 for those deposited at $P(O_2) = 100$ mTorr and $T_d = 600^\circ\text{C}$. Thus, by cross-plotting the breakdown field of the PLD titanium silicate films as a function of their corresponding refractive index, a linear correlation is obtained in Fig. 9(b). This linear correlation demonstrates the determin-

ing role of the porosity (or the film densification) on the breakdown voltage of the titanium silicate films.

IV. CONCLUSION

We have presented a comprehensive investigation on the effects of both oxygen background pressure and substrate deposition temperature on the growth of titanium silicate thin films from the pulsed-laser ablation of a TiO₂/SiO₂ composite target. The films are found to be amorphous although, at the highest T_d of 600 °C, some segregation starts to take place together with the formation of few anatase TiO₂ nanocrystallites. It is shown that $P(\text{O}_2)$ is a key factor in controlling both the morphology and the oxygen content of the silicate films. For $P(\text{O}_2) \geq 50$ mTorr, the films are porous and relatively rough, particularly at low T_d . In contrast, for low oxygen background pressures [i.e., $P(\text{O}_2) < 10$ mTorr down to vacuum], dense and smooth films are grown but they were found to be oxygen deficient. On the other hand, their post-annealing in O₂ atmosphere is demonstrated to be effective in bringing them back to their fully oxidized state. By achieving a systematic investigation of the electrical properties of these PLD titanium silicate films, we were able to point out two highly interesting correlations: (i) a strikingly strong exponential dependence of their room-temperature resistivity upon their oxygen content (over an impressive resistivity range as wide as 14 decades) and (ii) a direct linear correlation between their breakdown field and the porosity of the films (through the refractive index). Such correlations definitely represent key elements one has to consider for developing any theoretical model that aims at describing the conduction mechanisms of the PLD titanium silicate films. Finally, by combining the resistivity criterion with the dielectric characteristics, the films deposited under vacuum at $T_d = 600$ °C and postannealed under oxygen are definitely the best candidates which offer a combination of exceptional properties: a resistivity in excess of 10¹⁰ Ω cm, a k value of ~33, and a dissipation factor as low as ~0.01. Work is underway to investigate the integration of such titanium silicate films in advanced CMOS devices.

ACKNOWLEDGMENTS

This work was financially supported by MICRONET (the Network of Centers of Excellence on Microelectronic Devices, Circuits and Systems for ULSI) and the Natural Science and Engineering Research Council (NSERC) of Canada.

¹Semiconductor Industry Association, *The International Technology Roadmap for Semiconductors*, 2003 ed. (International SEMATECH, Austin, TX, 2003).

²G. D. Wilk, R. M. Wallace, and J. M. Anthony, *J. Appl. Phys.* **89**, 5243 (2001).

³F. Mondon and S. Blonkowski, *Microelectron. Reliab.* **43**, 1259 (2003).

⁴M. Kadoshima, M. Hiratani, Y. Shimamoto, K. Torii, H. Miki, S. Kimura, and T. Nabatame, *Thin Solid Films* **424**, 224 (2003).

⁵S. Ramanathan, C. M. Park, and P. C. McIntyre, *J. Appl. Phys.* **91**, 4521 (2002).

⁶A. Callegari, E. Cartier, M. Gribelyuk, H. F. Okorn-Schmidt, and T. Zabel, *J. Appl. Phys.* **90**, 6466 (2001).

⁷G. B. Alers, D. J. Werder, Y. Chabal, H. C. Lu, E. P. Gusev, E. Garfunkel, T. Gustafsson, and R. Urdahl, *Appl. Phys. Lett.* **73**, 1517 (1998).

⁸G. D. Wilk, R. M. Wallace, and J. M. Anthony, *J. Appl. Phys.* **87**, 484 (2000).

⁹G. D. Wilk and R. M. Wallace, *Appl. Phys. Lett.* **76**, 112 (2000).

¹⁰J. J. Chambers and G. N. Parsons, *J. Appl. Phys.* **90**, 918 (2001).

¹¹J. Zhu, Z. G. Liu, and Y. Feng, *J. Phys. D* **36**, 3051 (2003).

¹²G. Lucovsky and G. B. Rayner, Jr., *Appl. Phys. Lett.* **77**, 2912 (2000).

¹³G. B. Rayner, Jr., D. Kang, and G. Lucovsky, *J. Vac. Sci. Technol. B* **21**, 1783 (2003).

¹⁴P. H. Giauque, H. B. Cherry, and M.-A. Nicolet, *Microelectron. Eng.* **55**, 183 (2001).

¹⁵H. Demiryont, *Appl. Opt.* **24**, 2647 (1985).

¹⁶T. Nakayama, K. Onisawa, M. Fuyama, and M. Hanazono, *J. Electrochem. Soc.* **139**, 1204 (1992).

¹⁷D. K. Sarkar, E. Desbiens, and M. A. El Khakani, *Appl. Phys. Lett.* **80**, 294 (2002).

¹⁸D. Brassard, D. K. Sarkar, L. Ouellet, and M. A. El Khakani, *J. Vac. Sci. Technol. A* **22**, 851 (2004).

¹⁹A. Nishiyama, A. Kaneko, M. Koyama, Y. Kamata, I. Fujiwara, M. Koike, M. Yoshiki, and M. Koike, *Mater. Res. Soc. Symp. Proc.* **670**, K4.8.1 (2001).

²⁰T. Kamada, M. Kitagawa, M. Shibuya, and T. Hirao, *Jpn. J. Appl. Phys., Part 1* **30**, 3594 (1991).

²¹M. J. Alam and D. C. Cameron, *J. Sol-Gel Sci. Technol.* **25**, 137 (2002).

²²X. Gao and I. E. Wachs, *Catal. Today* **51**, 233 (1999).

²³X. Wang, H. Masumoto, Y. Someno, and T. Hirai, *Thin Solid Films* **338**, 105 (1999).

²⁴S.-M. Lee, J. H. Park, K.-S. Hong, W.-J. Cho, and D.-L. Kim, *J. Vac. Sci. Technol. A* **18**, 2384 (2000).

²⁵M. F. Ouellette, R. V. Lang, K. L. Yan, R. W. Bertram, and R. S. Owles, *J. Vac. Sci. Technol. A* **9**, 1188 (1991).

²⁶Y. Sorek, R. Reisfeld, I. Finkelstein, and S. Ruschin, *Appl. Phys. Lett.* **63**, 3256 (1993).

²⁷X. Orignac, D. Barbier, X. M. Du, and R. M. Almeida, *Appl. Phys. Lett.* **69**, 895 (1996).

²⁸D. Brassard, D. K. Sarkar, L. Ouellet, and M. A. El Khakani, *Appl. Phys. Lett.* **84**, 2304 (2004).

²⁹A. Paskaleva, A. J. Bauer, M. Lemberger, and S. Zürcher, *J. Appl. Phys.* **95**, 5583 (2004).

³⁰H. Sankur and W. Gunning, *J. Appl. Phys.* **66**, 4747 (1989).

³¹H. Sankur and W. Gunning, *J. Appl. Phys.* **66**, 807 (1989).

³²N. S. Gluck, H. Sankur, J. Heuer, J. DeNatale, and W. J. Gunning, *J. Appl. Phys.* **69**, 3037 (1990).

³³R. C. Smith, N. Hoilien, C. D. Stehpen, A. Campbell, J. T. Roberts, and W. L. Gladfelter, *Chem. Vac. Deposition* **9**, 79 (2003).

³⁴M. Atik and J. Zarzycki, *J. Mater. Sci. Lett.* **13**, 1301 (1994).

³⁵A. M. Seco, M. C. Gonçalves, and R. M. Almeida, *Mater. Sci. Eng., B* **B76**, 193 (2000).

³⁶M. A. El Khakani, B. Le Drogoff, and M. Chaker, *J. Mater. Res.* **14**, 3241 (1999) and references therein.

³⁷J. V. Grahn, M. Linder, and E. Fredriksson, *J. Vac. Sci. Technol. A* **16**, 2495 (1998).

³⁸S. Bordiga *et al.*, *J. Phys. Chem.* **98**, 4125 (1994).

³⁹T. Nakayama, *J. Electrochem. Soc.* **141**, 237 (1994).

⁴⁰I. Montero, L. Galàn, O. Najmi, and J. M. Albella, *Phys. Rev. B* **50**, 4884 (1994).

⁴¹R. P. Netterfield, P. J. Martin, C. G. Pacey, and W. G. Sainty, *J. Appl. Phys.* **66**, 1805 (1989).

⁴²B. Gallas, A. Brunet-Bruneau, S. Fisson, G. Vuye, and J. Rivory, *J. Appl. Phys.* **92**, 1922 (2002).

⁴³H. El. Omari, J. P. Boyeux, A. Errkik, M. Lemiti, and A. Laugier, *J. Appl. Phys.* **93**, 9803 (2003).

⁴⁴S. P. Murarka, *J. Vac. Sci. Technol.* **17**, 775 (1980).

⁴⁵P. Martin, M. Dufour, A. Ermolieff, S. Marthon, F. Pierre, and M. Dupuy, *J. Appl. Phys.* **72**, 2907 (1992).

⁴⁶C. Leung, M. Weinert, P. B. Allen, and R. M. Wentzcovitch, *Phys. Rev. B* **54**, 7857 (1996).

⁴⁷J. V. Mantese, W. A. Curtin, and W. W. Webb, *Phys. Rev. B* **33**, 7897 (1986).

⁴⁸S. Elliot, *The Physics and Chemistry of Solids* (Wiley, New York, 1998).

⁴⁹S.-J. Lee, K.-Y. Kang, and S.-K. Han, *Appl. Phys. Lett.* **75**, 1784 (1999).

⁵⁰A. Gutina, T. Antropova, E. Rysiakiewicz-Pasek, K. Vornik, and Yu. Feldman, *Microporous Mesoporous Mater.* **58**, 237 (2003).

⁵¹D. J. Taylor, P. F. Fleig, and S. L. Hietala, *Thin Solid Films* **332**, 257 (1998).